ELSEVIER

Polymer 41 (2000) 6833–6841

polymer

Plane stress essential work of fracture of 'pseudo-ductile' gelatin/maltodextrin biopolymer gel composites

K.P. Plucknett*, V. Normand

Unilever Research, Colworth Laboratory, Sharnbrook, Bedfordshire, MK44 1LQ, UK

Received 26 November 1999; accepted 10 January 2000

Abstract

Mixed biopolymer gels, comprised of spherical 'maltodextrin-rich' inclusions within a 'gelatin-rich' continuous matrix phase, have been shown to exhibit a form of 'pseudo-ductility' during tensile deformation, due to debonding of the inclusion/matrix interface during straining. A plane stress work of fracture technique, using thin sheet double edge notched tension (DENT) specimens, has been applied to these composites to assess the elastic and plastic contributions to crack growth during fracture. A transition from plane stress to mixed mode failure was observed to occur when the intact ligament length decreased below ~8*B* to 9*B* (where *B* is the sheet thickness). With the DENT technique, a specific *essential* work of fracture (elastic contribution) of ~110 J m^{-2} was calculated for the current gelatin/maltodextrin composition, under plane stress conditions.

Keywords: Biopolymers; Work of fracture; Gelatin

1. Introduction

There has recently been considerable emphasis placed upon understanding the large deformation behaviour of biopolymer gels, as they are subjected to such deformations in most applications (processing, consumption etc.) [1]. A range of single biopolymers have been examined, including; gelatin [2–4], agarose [5], starch [6], maltodextrin [7], gellan [8] and β-lactoglobulin [9]. Conversely, there are few studies on mixed biopolymer composite systems [10,11], although it is these materials that are ultimately of commercial interest.

It has recently been demonstrated that phase separated gelatin/maltodextrin composite gels can exhibit a 'pseudo-ductile' stress–strain response, with an *apparent* yield stress [11]. These gels are comprised of spherical 'maltodextrin-rich' inclusions within a continuous 'gelatin-rich' matrix phase. The apparent ductility arises from matrix/inclusion debonding under applied strain, which leads to the formation of an interfacial cavity, which subsequently grows. This process is largely reversible (prior to failure), due to the 'rubber-like' nature of gelatin, although some permanent strain is retained. This debonding behaviour is analogous to that in elastomeric composites, and an approximate interfacial fracture energy, G_c, can be calculated following Ref. [12] as;

$$\sigma_c^2 = 4\pi G_c E_m / 3r \quad (1)$$

where σ_c is the stress at which debonding occurs (in the present case this corresponds to the composite yield stress, σ_y, i.e. $\sigma_c = \sigma_y$), E_m the matrix elastic modulus and r the particle radius. For the present gelatin/maltodextrin composition, debonding initially occurs at ~27 kPa. Consequently, for a particle diameter of ~100 μm and matrix modulus of ~75 kPa, an interfacial fracture energy of ~0.25 J m^{-2} was measured at room temperature [11]. This is significantly lower than typically observed for immiscible homopolymers, without copolymer reinforcement (i.e. 1–5 J m^{-2}), but similar to adhesion energies between glassy polymers (i.e. 0.05–0.5 J m^{-2}) [13–16].

While the initial study on gelatin/maltodextrin composites assessed the fracture energy of the interface between the 'gelatin-rich' and 'maltodextrin-rich' phases [11], it does not address measurement of the 'toughness' of such materials in their bulk form. In the current work, a simple double edge notched tension (DENT) test is adapted for application to these materials, which has previously been used to determine the work of fracture of various metals and synthetic polymers [17–25].

* Corresponding author. Tel.: 44-1234-222482; fax.: 44-1234-222757.
E-mail address: kevin.plucknett@unilever.com (K.P. Plucknett).

0032-3861/00/$ - see front matter
PII: S0032-3861(00)00041-0

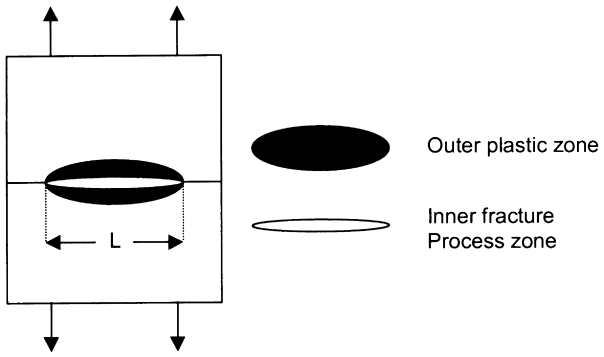

Fig. 1. Schematic diagram demonstrating both the fracture process zone and outer plastic zone in DENT test specimens.

2. Theoretical aspects

2.1. The essential work of fracture concept

Application of conventional fracture toughness testing methods to biopolymers is difficult, due largely to their low elastic modulus and tensile strength, which makes handling and gripping very difficult. As a consequence, a simple approach has been developed for tensile testing of biopolymer gels prepared as relatively thin sheets (i.e. ~1.4 mm thick), which was successfully applied to gelatin/maltodextrin composites [11]. This method entails 'sticking' the test specimen to the grip with double-sided tape, thus ensuring minimal handling damage. Broberg developed an analysis procedure for determination of the plane stress fracture energies of ductile materials using such a thin sheet test geometry [17–19], which has subsequently been adapted for ductile polymers [20–25]. This approach has been adopted in the current study for gelatin/maltodextrin mixed gels. Symmetrical notches are cut on both sides of a thin sheet specimen (to leave a ligament of length, L, with sheet thickness, B), that is then loaded in tension to failure (shown schematically in Fig. 1). Plane stress conditions can then be obtained when applying certain test specimen size criteria (discussed in the following section).

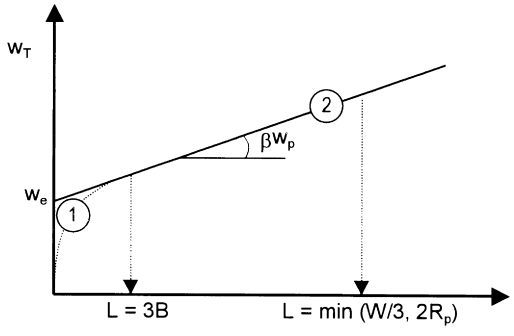

Fig. 2. Schematic representation of a plot of specific total work of fracture, w_T, against ligament length, L, demonstrating the regions of: (1) plane strain/plane stress; and (2) plane stress.

It has been stated that the non-elastic region at the crack tip comprises of an end region, where the fracture actually takes place, and an outer region, where plastic deformation is necessary to accommodate the strain in the end region [17,18]. This is shown schematically in Fig. 1. Based upon this analysis, the total work of fracture, W_T, can be separated into two principle components. The first is work consumed during the fracture process by neck formation and tearing, while the second is the work of plastic deformation. Typically, these contributions are referred to as the *essential*, W_e, and *non-essential*, W_p, work respectively. In addition, for polymeric samples, there is also an extra contribution to energy dissipation, or work, which is due to the viscoelastic nature of the material, W_v. The total work can therefore be seen as being the sum of these individual components;

$$W_T = W_e + W_p + W_v \tag{2}$$

For ligament length, L, and thickness, B, this relationship can then be rewritten for the *specific* total work as [22];

$$w_T = W_T/LB = w_e + (w_p V_p/LB) + (W_v/LB) \tag{3}$$

where $w_e = W_e/LB$, $w_p = W_p/L^2B$, V_p is the volume of the plastic deformation zone. w_e and w_p are the *specific essential* and *non-essential* work of fracture, respectively. It has been demonstrated that the plastic zone size can be given by [22];

$$V_p = \beta L^2 B \tag{4}$$

where β is a proportionality constant that is independent of the ligament length, L. If Eq. (4) is now substituted into Eq. (3), then [22];

$$w_T = w_e + \beta w_p L + (W_v/LB) \tag{5}$$

Typically, the viscoelastic contribution, W_v, is assumed to be negligible, and Eq. (5) simplifies to;

$$w_T = w_e + \beta w_p L \tag{6}$$

where the positive intercept at $L = 0$ gives the specific *essential* work of fracture, w_e, and the gradient of the curve provides a slope that is proportional to the specific *non-essential* work of fracture, w_p (i.e. the gradient, $m = \beta w_p$). A schematic representation of this type of plot is shown in Fig. 2.

2.2. Specimen size criteria for essential work of fracture testing

There are several specimen size criteria that need to be addressed for valid measurements of total work, W_T [19,26], particularly for ensuring the mode of applied stress (plane stress, mixed mode, etc.). To ensure conditions of plane stress, it is important that the ligament length, L, is significantly greater than the thickness of the specimen, B. When the ligament length approaches the specimen thickness, the stress state becomes mixed mode, having both plane strain/plane stress components. A number of authors have noted that, in the mixed mode region, w_T can vary non-linearly

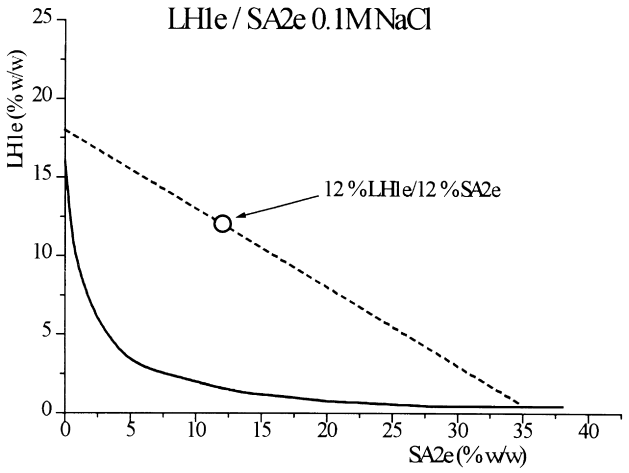

Fig. 3. The LH1e/SA2e phase diagram, showing the location of composition 12% LH1e/12% SA2e used in the present study.

with L [22,26], as shown schematically in Fig. 2. As a consequence, it has been suggested that the validity of Eq. (6) no longer holds. To avoid mixed mode effects, it is recommended that the measurements for determination of essential work of fracture are restricted to ligament lengths that are at least three to five times greater than the specimen thickness, i.e. [22,26];

$$L > 3B \text{ to } 5B \tag{7}$$

Hill has discussed a method for verifying the stress state for this type of notched test. In the plane stress region the DENT test specimen will yield at $\sim 1.15\sigma_y$ [27], while in the purely plane strain region of deformation, the DENT sample will yield at $\sim 2.97\sigma_y$ (where σ_y is the yield stress of the unnotched material).

In order to avoid any edge effects (i.e. to prevent yielding spreading to the lateral boundary of the specimen), it has been stated that the length of the ligament should be less than one third of the total specimen width, D, i.e. [19,20,22,26];

$$L < D/3 \tag{8}$$

Finally, the crack tip plastic zones should overlap to ensure that the ligament is fully yielded prior to crack growth, in order to maintain the proportionality of W_p with L^2 [19–22,26]. As a consequence of this requirement, the ligament length should be shorter than twice the plastic zone radius, R_p, around a single crack tip, i.e.;

$$L < 2R_p \tag{9}$$

For a circular plastic zone, the zone size can be estimated from;

$$2R_p = Ew_e/\pi\sigma_y^2 \tag{10}$$

while for a line plastic zone, the size can be estimated from;

$$2R_p = \pi Ew_e/8\sigma_y^2 \tag{11}$$

where E is the elastic modulus of the material.

In combination, it can be seen that these three basic restrictions on the ligament length lead to the following overall restriction on relative specimen dimensions [22];

$$3B \text{ to } 5B < L < \text{minimum}(D/3, 2R_p). \tag{12}$$

2.3. Procedure for determining crack opening displacement

Hashemi has outlined a methodology for indirectly determining the critical crack opening displacement (COD) [22]. This approach entails plotting the extension at failure, e_m, determined from the load/displacement curves, against ligament length. For the plane stress region, a linear relationship can be anticipated, of the form;

$$e_m = e_0 + e_pL \tag{13}$$

where e_0 is the extrapolated value at $L = 0$, and e_p can be viewed as the plastic contribution to extension. The intercept value, e_0, has been identified as being equivalent to the critical COD [17,28]. It was proposed that e_0 is related to the specific essential work of fracture, w_e, following Ref. [22] as;

$$w_e = e_0\sigma_y \tag{14}$$

which is analogous to the relationship proposed by Wells [29], between the true COD, δ, and the critical strain energy release rate, G_c, namely;

$$G_c = \delta\sigma_y. \tag{15}$$

3. Experimental procedures

3.1. Sample preparation

Lime hide gelatin (LH1e (pI = 4.6; M_n = 83,300 kDa; polydispersity = 1.77, measured by gas phase chromatography)), provided by SKW Biosystem (France), is a polypeptidic biopolymer obtained by alkaline degradation of collagen. LH1e solutions were prepared by dissolving the powder at 60°C for 30 min in de-ionised water. Sodium azide (~500 ppm) and sirius red (~500 ppm) were added to prevent bacteriological degradation and increase the gelatin fluorescence, respectively. When the solution is cooled below 28°C, a three-dimensional gel network appears, with the gelatin chains linked by triple helices. Maltodextrin (Paselli SA2e), supplied by Avebe (UK), is a polysaccharide obtained by enzymatic degradation of potato starch ($M_n = 6.2 \pm 0.5 \times 10^5$ Da; polydispersity = 1.45 ± 0.3, measured by light scattering) [30]. SA2e solutions were prepared by dissolving the powder in de-ionised water at 98°C for 30 min. On cooling below 31°C, the high molecular weight units initiate the condensation of the smallest chains and gel nucleation, forming a brittle, white gel.

Table 1
Predicted phase compositions for the gelatin/maltodextrin composite used in the current work (12% LH1e/12% SA2e), based upon Fig. 3

'Gelatin-rich' matrix phase	'Maltodextrin-rich' included phase
~18% LH1e/<0.1% SA2e	~0.5% LH1e/~35% SA2e

The gelatin/maltodextrin samples prepared in the current study are situated within the incompatibility domain of this system [31]. The location of the composition, 12% LH1e/12% SA2e, is plotted on the LH1e:SA2e:0.1 M NaCl phase diagram in Fig. 3, with predicted phase compositions given in Table 1. Composite samples were prepared by mixing the two biopolymer solutions at 60°C. The mixed solution was subsequently poured between parallel glass plates (covered with hydrophobic paper and separated by 1.4 mm spacers) and immersed in a controlled temperature water bath at 9°C.

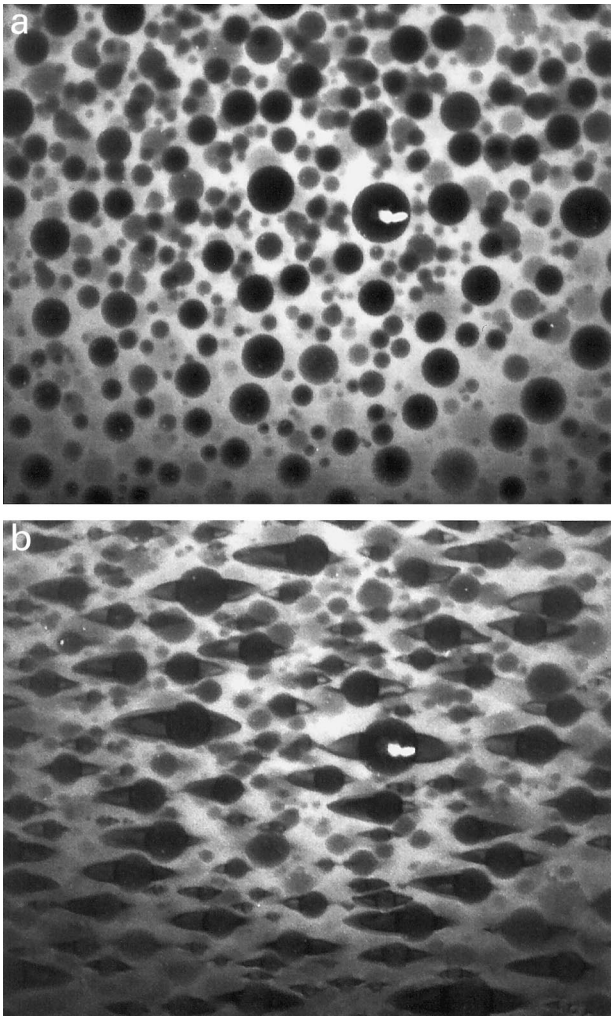

Fig. 4. *Dynamic* CLSM images of a tension test demonstrating the occurrence of interfacial debonding. Deformation strains, calculated using Eq. (17), are: (a) 0.0 strain units; (b) 0.51 (1.0 strain units is equivalent to 100% strain).

After quenching, the plates were stored at 5°C for 24 hours prior to use.

3.2. Mechanical testing procedures

Prior to mechanical testing, the gels were equilibrated at the test temperature (10°C for all tests). To avoid the typically encountered problems of specimen gripping when testing biopolymer gels (i.e. premature failure or irreversible damage), a very simple gripping approach was taken for the present work [11]. Tensile samples were cut from the 1.4 mm thick gel sheets using a 'dog-bone' shaped cookie cutter (60 mm gauge length × 6 mm width), and were then attached to card tabs using double-sided tape. The card tabs were then gripped on a mechanical test frame, with tests performed at a displacement rate of 100 mm min^{-1}. 'True' stress, σ_t, and 'true' strain, ϵ_t, were calculated following Ref. [32] as;

$$\sigma_t = F(L_0 + \Delta L)/(A_0 L_0) \tag{16}$$

$$\epsilon_t = \ln((L_0 + \Delta L)/L_0) \tag{17}$$

The tensile elastic modulus, E_t, can then be calculated as follows;

$$E_t = \sigma_t/\epsilon_t \tag{18}$$

A similar gripping procedure was also applied to the work of fracture tests, with rectangular samples cut from the cast gel sheets (dimensions of 80 mm × 50 mm × 1.4 mm). Symmetrical notches were then carefully cut into each side of the test pieces using a scalpel. It was not possible to produce test specimens with retained ligaments lengths of less than 4 mm, as the samples proved impossible to handle. However, as this ligament length is within the mixed mode region (i.e. theoretically a lower ligament limit of $3B$–$5B$ (i.e. 4.2–7.0 mm for the current samples)), this was not anticipated to be a problem. The test arrangement is similar to that shown in Fig. 1. Tests were performed at a displacement rate of 50 mm min^{-1}. The net section stress, σ_n, at failure, was calculated using;

$$\sigma_n = F/A_0. \tag{19}$$

3.3. Confocal laser scanning microscopy and dynamic failure visualisation

Dynamic mechanical tests were performed in situ on a confocal laser scanning microscope (CLSM), using a 'Minimat' tension/compression stage (Rheometric Scientific, Epsom, UK) [11]. Owing to the stage size constraints, 'dog-bone' shaped tension samples with a 30 mm gauge length and 3 mm sample width were used. 'Stepped' tensile displacements were used (typically 2 mm at 10 mm min^{-1}), to avoid stage vibration, with an image acquired after each 'step'. This procedure was repeated until the sample failed, after which further images were recorded of the relaxed structure.

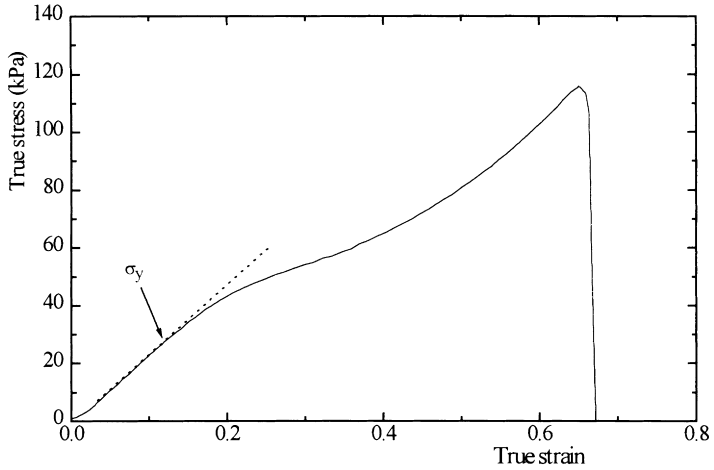

Fig. 5. Typical 'true' stress/'true' strain curve obtained for gelatin/maltodextrin composites (12% LH1e/12% SA2e), showing *apparent* yielding at ~27 kPa.

4. Results and discussion

4.1. Composite tensile behaviour and structure

A series of CLSM images of the structural evolution of the gelatin/maltodextrin composite with increasing applied strain is shown in Fig. 4 (measured at room temperature) [11]. The phase-separated nature of this material is readily evident, with spherical, included 'maltodextrin-rich' particles within a continuous matrix phase that is 'gelatin-rich' (Fig. 4a). Based upon phase diagram considerations, the volume fraction of included 'maltodextrin-rich' particles is ~0.33. Interfacial debonding occurs when the material is deformed above a strain of ~0.2 (or 20%), with subsequent 'cusp'-shaped void growth upon further straining (Fig. 4b). Qualitatively, it has been noted that the larger particles debond first, and debonding can be promoted at lower strains (i.e. ~0.125) when particles are in close proximity [11].

A typical corrected tensile 'true' stress/'true' strain curve is shown in Fig. 5. The material shows an *apparent* 'yielding' behaviour (i.e. reduced elastic modulus), with an average yield stress of ~27 kPa for these samples (defined as the initial point of deviation from linearity), that coincides with the interfacial debonding noted previously. Tensile failure stress varied between ~100 and 140 kPa, while the tensile elastic modulus was ~235 to 240 kPa. At high strains, once debonding has occurred, the gelatin matrix phase dominates the mechanical response as evidenced by the transition to strain-hardening behaviour (Fig. 5). Strain hardening was previously noted for 'pure' gelatin gels in both compression and shear [4], and also in the separated 'gelatin-rich' matrix phase of the present composition under tensile deformation [11].

4.2. Work of fracture determination

Typical load/displacement curves for the gelatin/maltodextrin composites, using the DENT test geometry, are shown in Fig. 6. The maximum load, maximum displacement

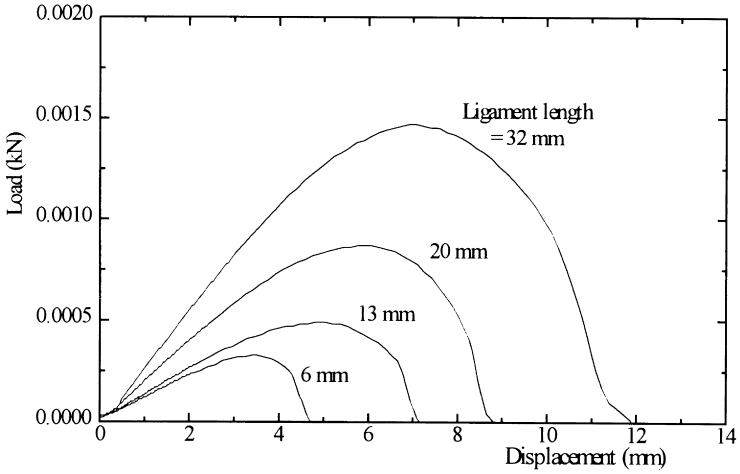

Fig. 6. Examples of typical load/displacement curves obtained for DENT tests conducted on gelatin/maltodextrin composites with various ligament lengths.

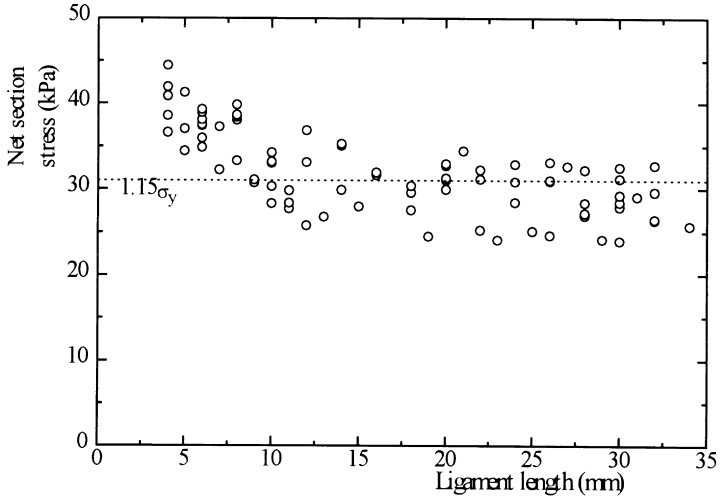

Fig. 7. The effects of ligament length upon the measured net-section stress.

and integrated area under the curve (total work) all increase with ligament length. An initially linear increase in load, with displacement, is observed. It is likely that the deviation from linearity indicates the onset of yielding (as noted in tensile tests), with the load decreasing when the notch starts to grow. This observation needs to be verified experimentally, to ensure that full ligament yielding occurs.

The effects of ligament length upon the net section stress, calculated using Eq. (19), are shown in Fig. 7. There is slightly more scatter in this data set than previously observed for DENT tests on synthetic polymers [20–25], which is believed to arise from slight regional variations in the average particle size and volume fraction. This is an artefact of sample preparation that is essentially impossible to remove. A high number of tests were conducted in the current work (i.e. $N = 83$), in order to minimise the observed effects of scatter, following the arguments outlined by Marchal et al [33]. The net section stress is higher for shorter ligament lengths (Fig. 7), as might be expected from theoretical considerations, and reaches a steady state condition for ligaments greater than ~12 to 13 mm. This can be seen to mark the transition from mixed mode to plane stress deformation, and occurs at ligament lengths corresponding to approximately 8*B*–9*B*, which is slightly higher than theory predicts, i.e. 3*B*–5*B* [19,26]. However, many of the studies previously conducted on polymeric materials have also shown that this transition occurs at ligament lengths significantly greater than predicted by theory [19,26], often reporting values as high as ~50*B* for polymers such as polycarbonate, poly(ether–ether ketone) and polyimide [22]. It has been predicted that, in the plane stress region, the DENT test specimen will yield (i.e. reach maximum net section stress) at ~1.15σ_y [27], where σ_y is the yield stress of the unnotched material. Conversely, in the plane strain region (i.e. when the ligament length is similar to the sample thickness), the DENT sample will yield at ~2.97σ_y. The

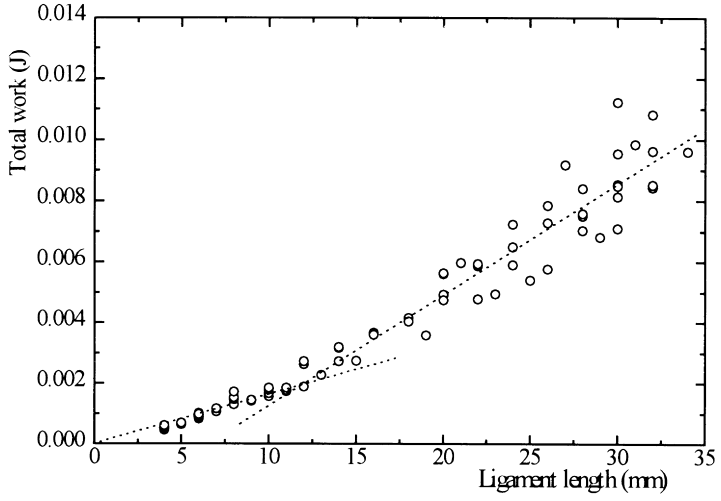

Fig. 8. The effects of ligament length upon the total work consumed during deformation.

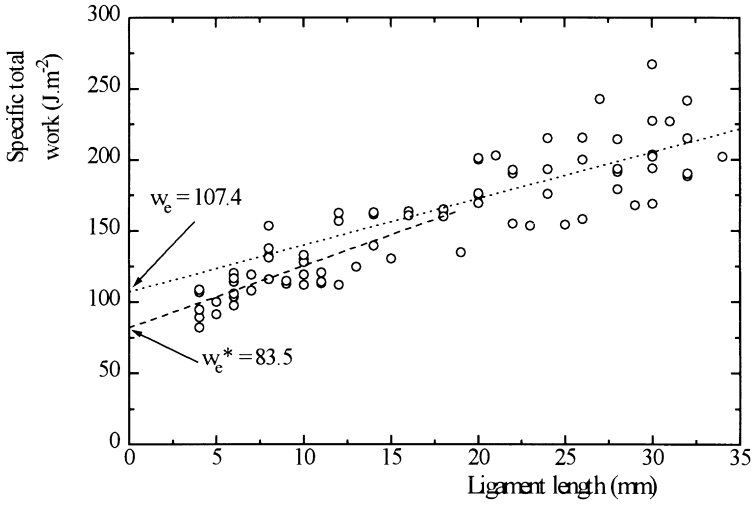

Fig. 9. The effects of ligament length upon the specific total work of fracture.

plane stress criteria for the gelatin/maltodextrin composite (i.e. $1.15\sigma_y = 1.15 \times 27$ kPa = ~31 kPa) is shown on Fig. 7 by the dotted line, and there is relatively good agreement with Hill's criteria for the plane stress region (i.e. for ligament lengths greater than ~12 to 13 mm). For lower ligament lengths, values of net section stress are greater than $\sim 1.15\sigma_y$, and tend towards $\sim 1.5\sigma_y$ as the ligament length approaches zero. In reality, the net section stress is likely to exceed $1.5\sigma_y$ after the transition from mixed mode to plane strain at low ligament lengths, in accordance with Hill [27], although it is not possible to verify this with the present material.

A plot of the total work consumed in deformation (obtained from the area under the load/displacement curve) as a function of ligament length is shown in Fig. 8. Two essentially linear regions are noted, indicating a similar transition to that observed in Fig. 7, occurring at a ligament length of ~12 to 13 mm. This again infers a change from mixed mode to purely plane stress deformation, as ligament length increases. If the curve of total work against ligament length is normalised (i.e. dividing by the ligament cross-sectional area), a plot of the specific total work against ligament length is obtained (Fig. 9). Applying a linear regression fit to this data, the *y*-axis intercept gives a value of the elastic work, w_e, while the gradient gives the plastic contribution, βw_p. Based upon data presented in Fig. 9, the plane stress values for w_e and βw_p were 107.4 ± 14.5 J m^{-2} and 3265 ± 582 J m^{-3}, respectively (Table 2). In the mixed mode region, the elastic work, w_e^*, is lower while the plastic work, βw_p^*, is higher, than for the plane stress region (Table 2), as would be expected theoretically [22,26].

Table 2
Values of specific essential and non-essential work of fracture measured in both the plane stress and mixed mode regions (*determined by extrapolation of data in the mixed mode region)

w_e (J m^{-2})	βw_p (J m^{-3})	w_e^* (J m^{-2})	βw_p^* (J m^{-3})
107.4 ± 14.5	3265 ± 582	83.5 ± 7.1	4253 ± 864

4.3. Comparison of measured work of fracture with alternative systems

The values of w_e and βw_p obtained in the present work are approximately three orders of magnitude less than those observed for ductile polymers (i.e. w_e ~20 to 70 kJ m^{-2}, βw_p ~1 to 7 MJ m^{-3}) [22]. However, it is interesting to note that the relative ratios of w_e:βw_p are similar. Fracture energies between ~0.1 and 6 J m^{-2} were noted for various β-lactoglobulin gels (depending upon the pH at which they were produced), using notched tension tests [9]. Whilst these values are one to two orders of magnitude less than the present gelatin/maltodextrin composites, it should be noted that the β-lactoglobulin gels exhibited significantly lower failure stresses and strains (i.e. from ~1 to 20 kPa for β-lactoglobulin, depending on synthesis route, against ~100 to 140 kPa for the present materials). Consequently, the effective work (i.e. area under the load/displacement curve) will be significantly lower for the β-lactoglobulin gels.

It is readily apparent that the fracture energy for the interface between the 'gelatin-rich' continuous phase and the 'maltodextrin-rich' included phase is significantly lower (i.e. ~0.25 J m^{-2}, measured at room temperature) than the composite fracture energy, w_e, measured using DENT tests (i.e. ~100 J m^{-2}). Although this discrepancy initially appears to be significant, it is actually similar to that often observed in synthetic polymer systems. One highly studied example is polystyrene (PS)/poly(methyl methacrylate) (PMMA). Both PS and PMMA alone typically exhibit fracture energies in the range of 400–2000 J m^{-2} [34,35] Conversely, in the absence of a 'bonding' block copolymer, the interfacial fracture energy is generally between ~5 and

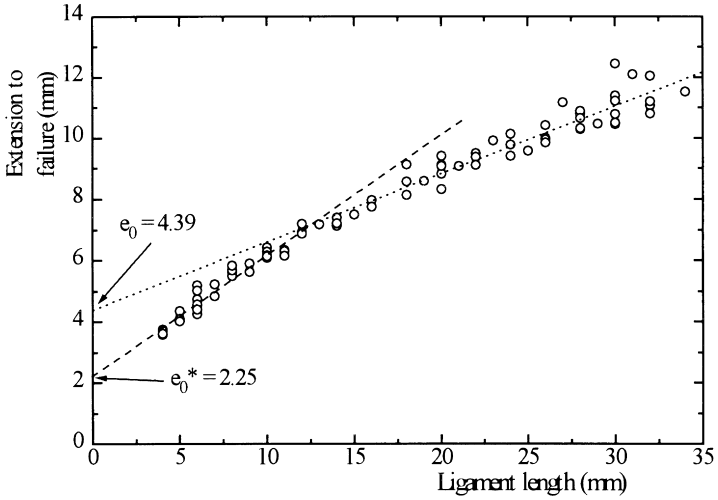

Fig. 10. The effects of ligament length upon extension to failure.

50 J m^{-2}, even after thermal 'welding' [36–38]. Another interesting example is the incompatible poly(propylene) (PP)/polyamide-6 (PA6) system. PP alone exhibits a fracture energy as high as 8000 J m^{-2} [34], while the interfacial fracture energy of the composite system can be varied between 1 and 100 J m^{-2} by careful control of the joining procedure [39].

4.4. Estimation of plastic zone size

Based upon the value obtained for w_e (i.e. 107.4 ± 14.5 J m^{-2}), it is possible to calculate the approximate zone size, $2r_p$, for either a circular or line plastic zone using Eqs. (10) and (11), respectively. In the present case (at 10°C), the composite tensile elastic modulus, $E \approx 240$ kPa, while the unnotched yield stress, $\sigma_y \approx 27$ kPa. This leads to calculated circular and line plastic zone sizes of ~11.1 ± 1.5 mm and ~13.6 ± 1.8 mm, respectively. If these values are applied in the specimen ligament size criteria outlined in Section 2.2, then it is apparent, from Eq. (12), that the minimum of $D/3$ or $2r_p$ will be the latter for the current material. However, it is also clear from Fig. 9 that a steady state condition is reached in the plane stress region (i.e. above ligament lengths of 12–13 mm) that continues to ligaments significantly longer than $D/3$ (i.e. 34 mm $\approx 2/3D$). In addition, the *average* net section stress in this region obeys theoretical expectations (i.e. the net section stress in the plane stress region $\approx 1.15\sigma_y$). It can therefore be inferred that the conditions applied in Eq. (12) are conservative. Similar observations have also been made in a number of other essential work of fracture studies [21,23], where the steady state plane stress region appeared to extend to ligament lengths as great as $3/4D$. The plastic zone sizes estimated in the current work are of a similar size to those determined for a synthetic polymer thought to be 'ideal' for DENT testing, such as amorphous copolyester [21,23].

Ultimately, it will be desirable to measure the plastic zone size using a direct method. A number of possible approaches can be envisaged to achieve this. Karger-Kocsis and co-workers have employed both post-fracture light microscopy and infra-red thermography techniques for a ductile copolyester [21,23–25]. Whilst the post-fracture light microscopy approach is unlikely to be suitable in the present case, due to strain relaxation, a dynamic strain mapping approach may be possible using a fiducial grid marked on the specimen surface in combination with video microscopy. This technique would provide distinct surface features whose deformation, relative to each other, could then be readily mapped. Similar approaches have been used in the past for examination of deformation and fracture of inorganic composites [40].

4.5. Estimation of crack opening displacement

Two distinct linear regions are apparent when plotting the extension at failure, e_m, against ligament length (Fig. 10). An observed transition from mixed mode to plane stress occurs at ligament lengths of ~12–13 mm, consistent

Table 3
A comparison of measured and estimated values of specific essential work of fracture. Estimated values of w_e and w_e^* are obtained using Eq. (14)

Estimated from extension to failure				Measured	
e_0 (mm)	w_e (J m^{-2})	e_0^* (mm)	w_e^* (J m^{-2})	w_e (J m^{-2})	w_e^* (J m^{-2})
4.39 ± 0.28	118.6 ± 7.5	2.25 ± 0.12	60.1 ± 3.4	107.4 ± 14.5	83.5 ± 7.1

with Figs. 7–9. Extrapolating from the plane stress region to the *y*-axis intercept (i.e. when $L = 0$), gives a value $e_0 \approx 4$ mm, with a value of $e_0^* \approx 2.5$ mm for the mixed mode region. Using Eq. (14) it is therefore possible to estimate w_e (and an equivalent w_e^* from the mixed mode region). These values are compared with those determined experimentally in Table 3. Given the approximate nature of this approach, particularly the fact that the values of e_0 and e_0^* are obtained from values of elongation to failure for the whole gauge length of the sample (initially 50 mm) for a relatively compliant material, and not simply around the notch region, there is relatively good agreement between the estimated and experimental values, especially for data in the plane stress region alone.

5. Conclusions

The plane stress essential work of fracture of a 'pseudo-yielding' biopolymer gel composite, gelatin/maltodextrin, has been measured using the DENT test, previously applied to metals and synthetic polymers. Debonding of the interface between the 'gelatin-rich' continuous matrix (low elastic modulus) and the 'maltodextrin-rich' included particles (high elastic modulus) occurs in this material, as it is deformed, resulting in the 'pseudo-yielding' response.

The DENT method involves cutting symmetrical notches on either side of a thin sheet rectangular test piece, of thickness *B*, to leave an intact ligament of material, which is then stressed in tension. A transition from plane stress to mixed mode (plane strain/plane stress) deformation occurs as the ligament length is reduced below $\sim 8B$ to $9B$. In the steady state plane stress region, the maximum net section stress was found to be close to the value predicted by theory, namely $\sim 1.15\sigma_y$ (where σ_y is the unnotched yield stress). In the mixed mode region, the maximum net section stress increased to $\sim 1.5\sigma_y$, and this value is predicted to increase to $\sim 2.97\sigma_y$ in the plane strain region.

Two linear regions were apparent on a plot of the total work consumed as a function of ligament length, marking a transition from plane stress to mixed mode deformation. The specific total work could then be determined by normalising this data with respect to the various ligament areas used. Extrapolation of the specific total work against ligament length curve to zero ligament length, then gave the specific *essential* work of fracture, w_e (for data solely from the plane stress region), which is the elastic contribution to failure in the process zone. The plastic contribution, termed the specific *non-essential* work of fracture, βw_p, can then be obtained from the gradient of this curve. In the present example, plane stress values of w_e and βw_p, were found to be 107.4 ± 14.5 J m^{-2} and 3265 ± 582 J m^{-3}, respectively.

Acknowledgements

The authors would like to thank Dudley Ferdinando for assistance with confocal microscopy, and Drs Stephen Pomfret, Bill Frith, Allan Clark and Ian Norton for valuable discussions regarding biopolymer gels.

References

[1] van Vliet T, Walstra P. Faraday Discuss 1995;101:359.
[2] Bagley EB, Wolf WJ, Christianson DD. Rheol Acta 1985;24:265.
[3] McEvoy H, Ross-Murphy SB, Clark AH. Polymer 1985;26:1483.
[4] Bot A, van Amerongen IA, Groot RD, Hoekstra NL, Agterof WGM. Polym Networks and Gels 1996;4:189.
[5] Hershko V, Nussinovitch A. J Texture Studies 1995;26:675.
[6] Luyten H, van Vliet T. J Texture Studies 1995;26:281.
[7] Chronakis IS. Crit Rev Food Sci 1998;38:599.
[8] Lelievre J, Mirza IA, Tung MA. J Food Engng 1992;16:25.
[9] Stading M, Hermansson AM. Food Hydrocolloids 1991;5:339.
[10] McEvoy H, Ross-Murphy SB, Clark AH. Polymer 1985;26:1493.
[11] Plucknett KP, Normand V, Pomfret SJ, Ferdinando D. Polymer 2000;41:2319.
[12] Gent AN. J Mater Sci 1980;15:2884.
[13] Creton C, Kramer EJ, Hui CY, Brown HR. Macromolecules 1992;25:3075.
[14] Kulasekere R, Kaiser H, Ankner JF, Russell TP, Brown HR, Hawker CJ, Mayes AM. Macromolecules 1996;29:5493.
[15] Gent AN, Shimizu N. J Appl Polym Sci 1986;32:5385.
[16] Mangipudi VS, Huang E, Tirrell M, Pocius AV. Macromol Symp 1996;102:131.
[17] Broberg KB. Int J Fracture Mech 1968;4:11.
[18] Broberg KB. J Mech Phy Solids 1971;19:407.
[19] Cotterell B, Reddel JK. Int J Fracture 1977;13:267.
[20] Hashemi S. Plastics. Rubber Comp Proc Appl 1993;20:229.
[21] Karger-Kocsis J. Polym Bull 1996;37:119.
[22] Hashemi S. J Mater Sci 1997;32:1563.
[23] Karger-Kocsis J, Czigány T, Moskala EJ. Polymer 1997;38:4587.
[24] Mouzakis DE, Stricker F, Mülhaupt R, Karger-Kocsis J. J Mater Sci 1998;33:2551.
[25] Karger-Kocsis J, Czigány T, Moskala EJ. Polymer 1998;39:3939.
[26] Saleemi AS, Narin JA. J Polym Engng Sci 1990;30:211.
[27] Hill R. J Mech Phys Solids 1952;1:19.
[28] Paton CA, Hashemi S. J Mater Sci 1992;27:2279.
[29] Wells AA. Br Welding J 1963;10:563.
[30] Defloor I, Vandrenreyken V, Grobet PJ, Delcour JA. J Chromatogr, A 1998;803:103.
[31] Normand V, Pudney PDA, Aymard P, Norton IT. J Appl Polym Sci 2000 (in press).
[32] Richards CW. Engineering materials science. Belmont, USA: Brooks/Cole, 1961.
[33] Marchal Y, Walhin JF, Delannay F. Int J Fracture 1997;87:189.
[34] Atkins AG, Mai YW. Elastic and plastic fracture: metals, polymers, ceramics, composites, biological materials. Chichester, UK: Ellis Horwood, 1985.
[35] Ward IM, Hadley DW. An introduction to the mechanical properties of solid polymers. Chichester, UK: Wiley, 1993.
[36] Foster KL, Wool RP. Macromolecules 1991;24:1397.
[37] Willet JL, Wool RP. Macromolecules 1993;26:5336.
[38] Brown HR, Krappe U, Stadler R. Macromolecules 1996;29:6582.
[39] Boucher E, Folkers JP, Hervet H, Léger L, Creton C. Macromolecules 1996;29:774.
[40] Poole WJ, Embury JD, MacEwen S, Kocks UF. Phil Mag A 1994;69:645.